Frequency Combs with Weakly Lasing Exciton-Polariton Condensates

K. Rayanov,[1] B. L. Altshuler,[1,2] Y. G. Rubo,[3] and S. Flach[1,4]

[1]*New Zealand Institute for Advanced Study, Centre for Theoretical Chemistry and Physics, Massey University, 0745 Auckland, New Zealand*

[2]*Physics Department, Columbia University, New York, New York 10027, USA*

[3]*Instituto de Energías Renovables, Universidad Nacional Autónoma de México, Temixco, Morelos 62580, Mexico*

[4]*Center for Theoretical Physics of Complex Systems, Institute for Basic Science, Daejeon 305-811, Korea*

(Received 10 January 2015; published 14 May 2015)

We predict the spontaneous modulated emission from a pair of exciton-polariton condensates due to coherent (Josephson) and dissipative coupling. We show that strong polariton-polariton interaction generates complex dynamics in the weak-lasing domain way beyond Hopf bifurcations. As a result, the exciton-polariton condensates exhibit self-induced oscillations and emit an equidistant frequency comb light spectrum. A plethora of possible emission spectra with asymmetric peak distributions appears due to spontaneously broken time-reversal symmetry. The lasing dynamics is affected by the shot noise arising from the influx of polaritons. That results in a complex inhomogeneous line broadening.

DOI: 10.1103/PhysRevLett.114.193901 PACS numbers: 42.55.Ah, 42.79.Hp, 71.36.+c, 78.67.-n

Condensation of exciton-polaritons (EPs) in semiconductor microcavities formed by two distributed Bragg mirrors with quantum wells between them has been experimentally observed [1–5]. Being incoherently excited in the microcavity, EP condensates are, in general, out of thermodynamic equilibrium. EP condensates refuel their particle depot from an excitonic reservoir and emit coherent light due to tunneling of the composite EP states through distributed Bragg mirrors. Sample inhomogeneity, either accidental or intentional, can induce several condensation centers (CCs) [3,6–8]. At low enough pumping, one expects a system of disconnected Bose-Einstein condensate (BEC) droplets emitting light at different uncorrelated frequencies. As the pumping increases, the condensates tend to establish mutual coherence and emit in a laser mode [6]. Already, two CCs can synchronize and emit at a single joint frequency [9,10]. This is possible because the condensates exchange particles due to Josephson coupling and adjust their emission frequencies. Those, in turn, depend on the number of condensed particles due to the polariton-polariton repulsion. In addition to the coherent Josephson coupling, the dissipative (radiative) coupling between CCs reflects the dependence of the losses in the system on the symmetry of single-particle states. A new stationary regime called weak lasing emerges when pumping rates reside between some minimal and maximal rates of losses [10]. In the weak lasing regime, the system is stabilized by the formation of specific many-particle states which adjust the balance between gain and loss in the system.

In this Letter, we show that, in the weak lasing regime, two CCs can emit not only at a single frequency, but also at a whole frequency comb which contains a great number of equidistant lines of coherent laserlike radiation. This emission reflects the fact of formation of spontaneous self-sustained anharmonic oscillations of both the occupation numbers and the relative phase between the condensates in sharp contrast to previously reported damped Josephson oscillations [11–13]. We study possible emission spectra and the way they are affected by noise. While the emission frequency of single-line EP lasers resides in the eV range [1,3,6,7,14], the modulation frequency of comb emission can be adjusted to be in the terahertz and microwave range. Filtering out of the high-frequency component through optical demodulation yields the low-frequency coherent signal as a new promising type of coherent terahertz emitter.

The EP self-induced oscillation is a novel mechanism of optical frequency comb generation. Its origin differs from that of mode-locked lasers [15,16], where the comb appears due to repetition of laser pulses. Also, contrary to the case of optical microresonators [17,18], the system is excited incoherently. We also note that EP comb generation relies on the presence of dissipative coupling between two lasing modes, contrary to the case of nonlinear distributed couplers [19,20] and multicore fiber systems [21]. The main benefit of the EP system is that the strong nonlinearity due to polariton-polariton repulsion results in the possibility of comb generation at relatively weak pumping, which is an important feature for optical computing and optical clock applications.

Consider two coupled EP condensates with order parameters

$$\psi_{1,2} = \sqrt{n_{1,2}}e^{i(\Phi\mp\phi)}, \tag{1}$$

where $n_{1,2}$ are the occupations of the two condensates, Φ is the total phase, and 2ϕ is the phase difference. The time evolution of $\psi_{1,2}$ is governed by the Langevin equations ($\hbar = 1$) [10]

$$\begin{aligned}\frac{d\psi_\mu}{dt} =& -\frac{1}{2}(g\psi_\mu + \gamma\psi_\nu)\\ &-\frac{\mathrm{i}}{2}(2\omega_\mu\psi_\mu - J\psi_\nu + \alpha|\psi_\mu|^2\psi_\mu) + f_\mu(t), \end{aligned}\quad (2)$$

where $\mu \neq \nu = 1, 2$ label the condensates. The parameter $g = \Gamma - W$ describes the difference between the rates of losses Γ and pumping W, ω_μ denotes the singe-particle energies of the condensates, the parameters γ and J define dissipative and coherent coupling between the condensates, respectively, and α is the polariton-polariton interaction constant. The last term in Eq. (2) is the Gaussian white noise satisfying $\langle f_\mu(t) f_{\mu'}\rangle = 0$ and $\langle f_\mu(t) f^*_{\mu'}(t')\rangle = W_\mu \delta_{\mu\mu'}\delta(t - t')$. Because of gauge invariance, only the frequency detuning ω is relevant, and in what follows, we will count the frequency from $\omega_0 = (\omega_1 + \omega_2)/2$. Rescaling time, we can fix $\gamma = 1$ and, since rescaling the condensate amplitudes is equivalent to a change of α, we can set $\alpha = 2$ without loss of generality.

The dissipative coupling makes the dissipation in the system dependent on the relative phase ϕ. This can be observed from the eigenvalues λ which control the condensate evolution $\psi_{1,2} \sim e^{\lambda t}$ in the absence of interaction. With increasing pumping (increasing γ/g), one of the eigenmodes turns unstable. Therefore, the dissipative coupling acts as a phase-selective pump which depends on the relative phase ϕ: it pumps one eigenmode while keeping the other one lossy. In this regime, nontrivial weak lasing states are formed.

First we consider the noise-free case, $f_{1,2} = 0$. Two nontrivial fixed-point solutions $F^\pm$ to Eqs. (2) characterized by nonzero time-independent triplets $\{n_1, n_2, \phi\}_\pm$ were identified (see Ref. [10] for a complete account). Here, we indicate that the total phase Φ of the condensates satisfies

$$\dot{\Phi} = \left(-\frac{1}{2} + \frac{J\cos(2\phi)}{4\sqrt{n_1 n_2}}\right)(n_1 + n_2) + \frac{\sin(2\phi)}{4\sqrt{n_1 n_2}}(n_1 - n_2), \quad (3)$$

and the rhs in (3) gives a time-independent frequency $\dot{\Phi} = -\Omega_0$ at $F^\pm$. The two centers evolve in a coherent fashion $\psi_{1,2} \sim \mathrm{e}^{-i\Omega_0 t}$ and Ω_0 defines the blueshift of the emission line with respect to the average single-particle frequency. We note that $F^\pm$ correspond to fixed point solutions in the subspace $\{n_1, n_2, \phi\}_\pm$, while they are limit cycles (LCs) (periodic orbits) in the full four-dimensional space $\{\psi_1, \psi_2\}$. The $F^\pm$ states lose stability at $g = g_c^\pm$ [10]

$$2(g_c^4 + J^2)R^\pm(g_c) = (g_c^2 + 1)[\omega g_c + (g_c^2 + J^2)R^\pm(g_c)], \quad (4)$$

where $R^\pm(g) = \pm\sqrt{(1 - g^2)/(g^2 + J^2)}$. We plot the two instability curves in the $\{g, \omega\}$ space at fixed $J = 0.1$ in Fig. 1 (solid lines). The $F^\pm$ states are unstable in the shaded areas LC$^\pm$. In particular, they are both unstable in the joint area LC$^+$ and LC$^-$, where the trivial solution $n_1 = n_2 = 0$ is unstable as well. What are, then, the stable stationary states of the system, if any?

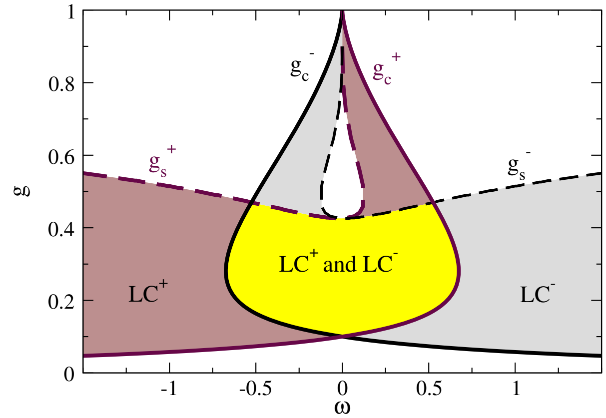

FIG. 1 (color online). Limit cycles LC$^\pm$ appear in the shaded areas in the ω, g-parameter space. Stable LC$^\pm$ are born through Hopf bifurcations at the solid $g_c^\pm$ line and turn unstable at the dashed $g_s^\pm$ lines where they undergo period doubling bifurcations. They are the only stable attractors to coexist in the central (yellow) region. Here, $J = 0.1\gamma$.

The answer is obtained by linearizing the phase space flow around $F^\pm$ in the subspace $\{n_1, n_2, \phi\}_\pm$. At $g = g_c^\pm$, two corresponding eigenvalues are purely imaginary $\pm i\Delta\Omega$, with their real parts changing sign. As a result, a supercritical Hopf bifurcation occurs, where stable limit cycles LC$^\pm$ with frequency

$$\Delta\Omega = \sqrt{2g^2 + J^2/g^2 + J^2 + \omega g/R^\pm} \quad (5)$$

are born around the respective unstable fixed points $F^\pm$ [22].

Away from the bifurcation line, the LCs increase the oscillation amplitudes, deform, and change their frequency. The coexistence region of LC$^+$ and LC$^-$ grows in size as the Josephson tunneling is reduced. At the Hopf bifurcation, where a LC emerges, $n_{1,2}, \phi$, and $\dot{\Phi}$ become periodic functions of time with period $T = 2\pi/\Delta\Omega$. The nonzero average of $\dot{\Phi}$ results in a linear time dependence, $\Phi_{\mathrm{DC}} = -\Omega_0 t$, similar to $F^\pm$. Therefore,

$$\psi_\mu(t) = p_\mu(t)e^{-i\Omega_0 t}, \quad (6)$$

where the functions $p_\mu(t) = p_\mu(t + T)$ are periodic in time. The Fourier spectrum of $\psi_\mu(t)$ is an equidistant array of peaks with frequency harmonics positioned at $\Omega_0 + N\Delta\Omega$.

Approaching the dashed lines $g_s^\pm$ in Fig. 1, the corresponding LC turns unstable and undergoes a period doubling bifurcation. This gives rise to a new stable period-doubled LC, which, however, again quickly undergoes a period doubling bifurcation. A period doubling route to chaos along a Feigenbaum scenario leads to chaotic attractors [23]. Therefore, just two coupled exciton-polariton condensates suffice to produce an extremely rich and complex synchronized dynamics.

Experimentally, the polariton order parameter is detected by analyzing the emitted light from the microcavity. In near-field measurements, only small parts of the sample, like one condensation center, can be probed. Our aim is to calculate the spectral density $I_{1,2}(\Omega)$ of the radiation corresponding to different nontrivial attractors. Applying a Fourier transformation (FT) we have

$$I_\mu(\Omega) = |\mathrm{FT}[z_\mu(t)]|^2, \qquad \mu = 1,2. \tag{7}$$

In the fixed points $F^\pm$, $\dot{n}_{1,2} = \dot{\phi} = 0$, and the time dependence comes from the evolution of the total phase $\Phi = -\Omega_0 t$

$$\psi_\mu(t) = C_\mu e^{-i\Omega_0 t}, \tag{8}$$

with constants C_μ. Thus, the condensates emit light at frequency Ω_0 fully synchronized. The emission spectrum consists of only one peak, in contrast to the case of non-interacting polaritons, where two separated peaks are expected.

Since the limit cycles $\mathrm{LC}^\pm$ are characterized by an equidistant spectrum, first, we numerically compute the corresponding frequency positions, and then, calculate the intensity of each frequency harmonics. The resulting spectra are shown in Figs. 2(a) and 2(b). Close to the Hopf bifurcation, there is only one considerable emission peak originating from the F^+ spectral line [Figs. 2(a) and 2(b) upper panels]. Further away from the Hopf bifurcation, the satellite peaks grow to form a frequency comb with asymmetric tails [Figs. 2(a) and 2(b) lower panels]. The comb also acquires several peak maxima, with the highest peak originating from a satellite with nonzero $N = 2$ [Figs. 2(a) and 2(b) lower panels]. When the LC undergoes a period doubling bifurcation, the comb becomes twice as dense [Fig. 2(c)].

The typical modulation frequency is independent of the polariton-polariton interaction constant α and is of the order of the coupling constant $\Delta\Omega \sim \gamma \sim 1$ meV. This puts the typical comb spacing just below the terahertz region. One can achieve terahertz modulation in the microcavities with a lower quality factor and/or for finite detuning ω [see Eq. (5)]. On the other hand, $\Delta\Omega$ is shifted into the millimeter-wave band for high-quality microcavities and due to the reduction of separation by period doubling.

Finally, we consider the influence of noise in Eq. (2). In general, it will broaden the peaks discussed so far, and can lead to a merging of peaks with too small spacing. The emission spectrum can be obtained using the Wiener-Khinchin theorem

$$I_\mu(\Omega) = \frac{1}{\pi}\Re\int_0^\infty \langle\psi_\mu(t)\psi_\mu^*(0)\rangle e^{i\Omega t}dt, \tag{9}$$

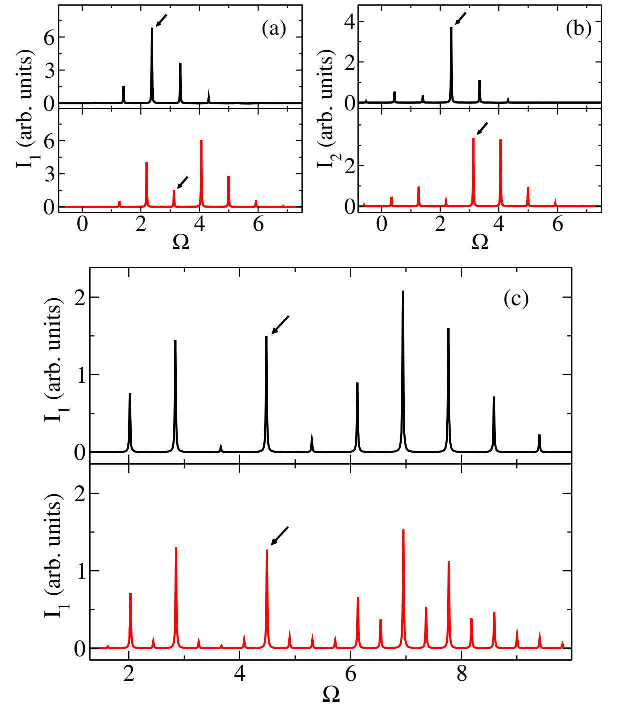

FIG. 2 (color online). Asymmetric frequency combs in the near-field spectrum from a LC^+ (a),(b) and a period doubled LC^+ (c). Here, $\omega = 0$, $J = 0.1$. The small arrows indicate the position of the respective $N = 0$ peak. (a) I_1 with $g = 0.19$ (upper panel), $g = 0.27$ (lower panel). (b) The same as (a) but for I_2. (c) I_1 for $g = 0.425$ (upper panel) and $g = 0.426$ (lower panel, period doubled LC spectrum). For visualization, a small artificial Lorentzian line width was added to all emission lines.

where $\langle\psi_\mu(t)\psi_\mu^*(0)\rangle$ is the autocorrelation of the, now, random process $\psi_\mu(t)$.

The $F^\pm$ states are periodic orbits in the full four-dimensional phase space, and the dynamics along these periodic orbits is parametrized by the total phase Φ. While fluctuations off the periodic orbit will relax back, fluctuations along the orbit do not, and will enforce diffusion of Φ on the orbit. The latter fluctuations form a Lorentzian line with the full width at half maximum (FWHM) given by $W(n_1 + n_2)/8n_1n_2$ [24]. Note that the FWHM is inversely proportional to the number of particles in the condensate, as it should be for a laser.

In contrast to the $F^\pm$ states, the $\mathrm{LC}^\pm$ states are formed by the motion on a two-dimensional torus in the full phase space. The stability of the attractor demands that fluctuations off the torus relax back. Fluctuations along the torus surface enforce a diffusion on it. The two nontrivial phases which diffuse, are the total phase Φ and the LC phase.

Close to the Hopf bifurcation, and in the presence of only a few satellite peaks, we can obtain a closed formula for the line width. To parametrize the LC, we consider two time arguments, one originating from the total phase and the other from the LC phase. Time evolution of the former defines the global blueshift of the emission lines, while the latter is responsible for the formation of the frequency comb. Noise in both arguments broadens the emission lines. According to Eq. (6), we have

$$\psi_\mu(t) = p_\mu\left(t + \frac{1}{-v(t)}\int P(\tau)d\tau\right)e^{-i\Omega_0 t + i\int F(\tau)d\tau}$$
$$= \sum_N C_\mu^N e^{-iN\Delta\Omega\{t+[1/-v(t)]\int P(\tau)d\tau\}} e^{-i\Omega_0 t + i\int F(\tau)d\tau}, \tag{10}$$

where the periodic function p_μ has been expanded in a Fourier series with coefficients C_μ^N, $N = 0, \pm 1, \pm 2, \ldots$, and $v(t)$ is the velocity of the noise-free trajectory along the LC in the three-dimensional space $\{n_1, n_2, \phi\}$. $P(t)$ is the projected noise along the LC, while $F(t) = (1/4\mathrm{i})[\sum_\mu [f_\mu(t)/\psi_\mu] - \mathrm{c.c.}]$ is the noise added to the rhs of Eq. (3) for $\dot{\Phi}$. Since $\Phi(t)$ is time periodic, perturbing the time argument of $p_\mu(t)$ already accounts for a part of the noise $F(t)$. The transformation of the LC frequency comb into the single line emission through the Hopf bifurcations happens through a continuous decaying and washing out of the satellite peaks. Therefore, the periodic part of $\Phi(t)$ is negligible compared to its DC part, and the above separation of noise in the time arguments is justified.

The two noise terms possess nonvanishing correlations

$$\langle [NP(t) + F(t)][NP(t') + F(t')]\rangle = 2\kappa_N(t)\delta(t - t'), \tag{11}$$

where denoting $\langle P(t)P(t')\rangle = \kappa_{PP}\delta(t - t')$, $\langle F(t)F(t')\rangle = \kappa_{FF}\delta(t - t')$, $\langle P(t)F(t')\rangle = \kappa_{PF}\delta(t - t')$, we have

$$\kappa_N = \kappa_{FF} + 2N\kappa_{PF} + N^2\kappa_{PP}, \tag{12}$$

with an asymmetric (blueshifted vs redshifted) dependence on the comb line number N, originating in the broken time-reversal symmetry of the dissipative dynamics. The nonzero cross correlations and the asymmetry reflect the fact that both the noise of the global phase and the noise of the preexponential factor affect the width of the comb lines in comparable and nonadditive ways under conditions when the overlap of the lines becomes substantial.

The intensity of the noise $\kappa_N(t)$ is periodic in time, which originates from the oscillation of occupation numbers and the relative phase for evolution along the LC. Experimentally, the measurement time spans many LC periods and one can use the average value $\bar{\kappa}_N = (1/T)\int_0^T \kappa_N(\tau)d\tau$. Then,

$$I_\mu(\Omega) = \frac{1}{\pi T}\sum_N |C_\mu^N|^2 \frac{\bar{\kappa}_N}{\bar{\kappa}_N^2 + (\Omega - \Omega_0 - N\Delta\Omega)^2}. \tag{13}$$

The result is a Lorentzian for every emission line, with an N-dependent width $\bar{\kappa}_N$ according to Eq. (11). The N dependence of the line broadening $\bar{\kappa}_N$ follows from Eq. (12) and shows two remarkable features. First, there is a symmetric line broadening $\sim N^2$ which dominates for large N. Second, there is an asymmetric contribution $\sim N$ which originates from nonzero correlations κ_{PF}. It may lead to a satellite peak with $N \neq 0$ becoming more narrow than the main peak $N = 0$, and can further enhance the asymmetry of the spectrum, as compared to the noise-free case.

To calculate the line width $\bar{\kappa}$ numerically, we denote by $(A(t), B(t), C(t))^\mathrm{T}$ the normalized tangent vector along the LC in the coordinates $(\phi, n_1, n_2)^\mathrm{T}$. Then, P is the noise in $\dot{\phi}, \dot{n}_1, \dot{n}_2$ projected onto this tangent and we can evaluate from Eq. (11)

$$\kappa_N = \frac{W_1}{n_1}\left[N^2\left(\frac{A^2}{4} + B^2 n_1^2\right) - \frac{NA}{4} + \frac{1}{16}\right]$$
$$+ \frac{W_2}{n_2}\left[N^2\left(\frac{A^2}{4} + C^2 n_2^2\right) + \frac{NA}{4} + \frac{1}{16}\right]. \tag{14}$$

We show the spectrum with inhomogeneous line broadening compared to the noise-free case in Fig. 3. Because of noise, the asymmetry of the spectrum is enhanced and the strict equidistance of emission lines is relaxed for strong enough line broadening.

The analysis of modulated emission from a pair of condensation centers sheds light on features of exciton-polariton lasing from disordered microcavities, where physics is determined by optimal configurations which consist of only two localized states resonantly coupled with each other, as the probability to have coupling with more states vanishes. Therefore, one expects to observe the frequency comb lasing from disordered microcavities as well. The features of the modulated emission discussed above are very reminiscent of some of the experimentally obtained spectra. In particular, equidistant peaks with a gradual increase of the line width of satellite peaks were reported in Fig. 2(b) of Ref. [7] and Fig. 1 of Ref. [14]. More analysis is needed to make definite conclusions.

To achieve and manipulate the comb generation, it is convenient to operate with the polariton condensates that are decoupled from the exciton reservoirs created by

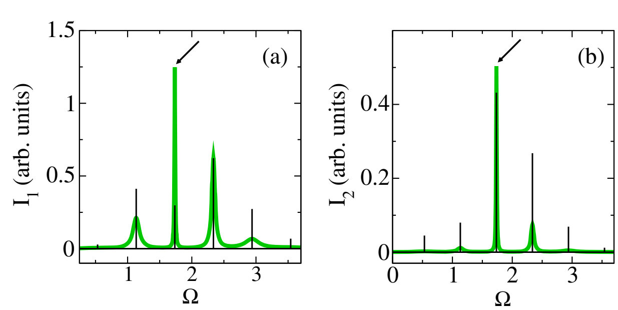

FIG. 3 (color online). Noisy (green lines) against noise-free (black frequency combs) spectrum of a LC$^+$ at $g = 0.7$, $\omega = 0$, $J = 0.5$, for (a) condensation center 1 and (b) condensation center 2. The arrows indicate the central peak. Here, $W = 0.02$.

external pumping. Formation of such "trapped" condensates has been recently reported [25]. Owing to the presence of dissipative coupling between the condensates [26], low threshold pumping powers (∼10 mW for a single trapped condensate), and feasible adjustments of condensate geometry, this distributed system is a promising candidate for the frequency comb generation discussed in this Letter.

Dissipative coupling between coexisting exciton-polariton condensates in semiconductor microcavities, together with a strong polariton-polariton repulsion, leads to a rich dissipative nonlinear dynamics already for two coupled condensates. We showed that, in addition to full synchronization [9,10], formation of limit cycles gives rise to frequency combs of equidistant asymmetric spectral lines. The frequency offset and line spacing of the combs are tunable through the control parameters. Through period doubling, the line spacing can be additionally reduced by an order of magnitude. This modulated emission can be useful for terahertz and microwave applications. Shot noise from the pump results in a complex diffusion in phase space and has a strong impact on higher order satellite peaks.

We thank I. Aleiner and A. Kavokin for valuable discussions. Y. G. R. acknowledges support from the EU FP7 IRSES Project POLAPHEN and from CONACYT under the Grant No. 251808.

[1] J. Kasprzak, M. Richard, S. Kundermann, A. Baas, P. Jeanbrun, J. M. J. Keeling, F. M. Marchetti, M. H. Szymańska, R. André, J. L. Staehli, V. Savona, P. B. Littlewood, B. Deveaud, and L. S. Dang, Nature (London) **443**, 409 (2006).
[2] R. Balili, V. Hartwell, D. Snoke, L. Pfeiffer, and K. West, Science **316**, 1007 (2007).
[3] C. W. Lai, N. Y. Kim, S. Utsunomiya, G. Roumpos, H. Deng, M. D. Fraser, T. Byrnes, P. Recher, N. Kumada, T. Fujisawa, and Y. Yamamoto, Nature (London) **450**, 529 (2007).
[4] J. J. Baumberg, A. V. Kavokin, S. Christopoulos, A. J. D. Grundy, R. Butté, G. Christmann, D. D. Solnyshkov, G. Malpuech, G. Baldassarri Höger von Högersthal, E. Feltin, J.-F. Carlin, and N. Grandjean, Phys. Rev. Lett. **101**, 136409 (2008).
[5] E. Wertz, L. Ferrier, D. D. Solnyshkov, P. Senellart, D. Bajoni, A. Miard, A. Lemaître, G. Malpuech, and J. Bloch, Appl. Phys. Lett. **95**, 051108 (2009).
[6] A. Baas, K. G. Lagoudakis, M. Richard, R. André, L. S. Dang, and B. Deveaud-Plédran, Phys. Rev. Lett. **100**, 170401 (2008).
[7] D. N. Krizhanovskii, K. G. Lagoudakis, M. Wouters, B. Pietka, R. A. Bradley, K. Guda, D. M. Whittaker, M. S. Skolnick, B. Deveaud-Plédran, M. Richard, R. André, and L. S. Dang, Phys. Rev. B **80**, 045317 (2009).
[8] N. Y. Kim, K. Kusudo, C. Wu, N. Masumoto, A. Löffler, S. Höfling, N. Kumada, L. Worschech, A. Forchel, and Y. Yamamoto, Nat. Phys. **7**, 681 (2011).
[9] M. Wouters, Phys. Rev. B **77**, 121302 (2008).
[10] I. L. Aleiner, B. L. Altshuler, and Y. G. Rubo, Phys. Rev. B **85**, 121301 (2012).
[11] D. Sarchi, I. Carusotto, M. Wouters, and V. Savona, Phys. Rev. B **77**, 125324 (2008).
[12] I. A. Shelykh, D. D. Solnyshkov, G. Pavlovic, and G. Malpuech, Phys. Rev. B **78**, 041302 (2008).
[13] K. G. Lagoudakis, B. Pietka, M. Wouters, R. André, and B. Deveaud-Plédran, Phys. Rev. Lett. **105**, 120403 (2010).
[14] A. P. D. Love, D. N. Krizhanovskii, D. M. Whittaker, R. Bouchekioua, D. Sanvitto, S. A. Rizeiqi, R. Bradley, M. S. Skolnick, P. R. Eastham, R. André, and L. S. Dang, Phys. Rev. Lett. **101**, 067404 (2008).
[15] Th. Udem, R. Holzwarth, and T. W. Hänsch, Nature (London) **416**, 233 (2002).
[16] S. T. Cundiff and J. Ye, Rev. Mod. Phys. **75**, 325 (2003).
[17] P. Del'Haye, A. Schliesser, O. Arcizet, T. Wilken, R. Holzwarth, and T. J. Kippenberg, Nature (London) **450**, 1214 (2007).
[18] T. J. Kippenberg, R. Holzwarth, and S. A. Diddams, Science **332**, 555 (2011).
[19] S. M. Jensen, IEEE J. Quantum Electron. **18**, 1580 (1982).
[20] A. A. Maier, Phys. Usp. **39**, 1109 (1996).
[21] A. M. Rubenchik, E. V. Tkachenko, M. P. Fedoruk, and S. K. Turitsyn, Opt. Lett. **38**, 4232 (2013).
[22] These new solutions are limiting two-dimensional tori in the full four-dimensional space $\{\psi_1, \psi_2\}$, which will become particularly important in the presence of noise.
[23] N. V. Alexeeva, I. V. Barashenkov, K. Rayanov, and S. Flach, Phys. Rev. A **89**, 013848 (2014).
[24] See Supplemental Material at http://link.aps.org/supplemental/10.1103/PhysRevLett.114.193901 for the derivation of the Lorentzian line width.
[25] P. Cristofolini, A. Dreismann, G. Christmann, G. Franchetti, N. G. Berloff, P. Tsotsis, Z. Hatzopoulos, P. G. Savvidis, and J. J. Baumberg, Phys. Rev. Lett. **110**, 186403 (2013).
[26] H. Ohadi, R. L. Gregory, T. Freegarde, Y. G. Rubo, A. V. Kavokin, and P. G. Lagoudakis, arXiv:1406.6377.